

On the orbital decay of the PSR J0045-7319 Binary

Pawan Kumar*

Institute for Advanced Study, Princeton, NJ 08540

and

Eliot J. Quataert

Harvard-Smithsonian Center for Astrophysics, 60 Garden St., Cambridge, MA 02138

ABSTRACT

Recent observations of PSR J0045-7319, a radio pulsar in a close eccentric orbit with a massive main sequence B-star companion, indicate that the system's orbital period is decreasing on a timescale $\sim 5 \times 10^5$ years (Kaspi et al. 1996). Timing observations of PSR J0045-7319 also indicate that the B-star is rotating rapidly, perhaps close to its breakup rotation rate (Lai et al. 1995, Kaspi et al. 1996). For rapid (super-synchronous) prograde rotation of the B-star, tidal dissipation leads to an increasing orbital period for the binary system, while for retrograde rotation of any magnitude, the orbital period decreases with time. We show that if tidal effects are to account for the observed orbital decay of the PSR J0045-7319 binary, the B-star must have retrograde rotation. This implies that the supernova that produced the pulsar in this binary system likely had a dipole anisotropy.

For a reasonably wide range of retrograde rotation rates, the energy in the dynamical tide of the B-star needs to be dissipated in about one orbital period in order to account for the observed orbital evolution time for the PSR J0045-7319 binary. We show, however, that the radiative dissipation of the dynamical tide in a rigidly rotating B-star is too inefficient by a factor of $\approx 10^3$, regardless of the magnitude of the rotation rate. We describe how, when the surface of the B-star is rotating nearly synchronously (which is expected from the work of Goldreich and Nicholson, 1989), the energy in the dynamical tide is dissipated in less than an orbital period, thus reconciling the theoretical and observed rates of orbital evolution.

Nonlinear parametric decay of the equilibrium tide, for rigid retrograde rotation of the B-star, may also be able to explain the observed rate of orbital evolution, though the margin of instability is too small to draw definitive conclusions about the relevance of this process for the PSR J0045-7319 Binary.

Subject headings: stars: binaries — stars: oscillations — stars: rotation — stars: early-type pulsars: individual (PSR J0045-7319)

*Alfred P. Sloan Fellow & NSF Young Investigator

email addresses: pk@sns.ias.edu (P. Kumar)

equataert@cfa.harvard.edu (E.J. Quataert)

§1. Introduction

The recent discovery of two radio pulsars in binary systems with main sequence star companions has provided the opportunity to study tidal interactions with unprecedented precision (McConnell et al. 1991, Kaspi et al. 1994; Johnston et al. 1992). Of these two radio pulsars, the one in the Small Magellanic Cloud (SMC), PSR J0045-7319 (which has a spin period of 0.93 s), is particularly interesting for studying tidal interactions because the periastron separation between the neutron star and its companion, a main sequence B-star of mass $\approx 8.8M_{\odot}$, is only about 4 times the B-star radius. The monitoring of pulse arrival times for the SMC pulsar has enabled accurate determination of several orbital parameters such as the period (51 days), eccentricity (0.808) and their time derivatives. Kaspi et al. (1996) report that the orbital period for the PSR J0045-7319 Binary is decreasing on a time scale of $\sim 5 \times 10^5$ years and that the orbital eccentricity is probably evolving more slowly. All relevant parameters for this system are included in table 1 for easy access. The work of Lai et al. (1995), Kaspi et al. (1996) and Bell et al. (1995) has also provided evidence that the B-star companion is rotating close to its break-up rotation rate and that its spin axis is misaligned with the angular momentum of the system.

The evolution time for the SMC Binary's orbit due to the radiative dissipation of the dynamical tide (in a nonrotating B-star) is $\sim 10^9$ years (see §2). It has been suggested (Lai, 1996), however, that the observed rapid evolution of the SMC Binary can be accounted for by the radiative dissipation of the dynamical tide, provided that the B-star companion to PSR J0045-7319 has a rapid retrograde rotation rate of $\hat{\Omega}_* \approx -0.4$, where $\hat{\Omega}_*$ is the component of the stellar rotation rate perpendicular to the orbital plane in units of $(GM_*/R_*^3)^{1/2}$. Retrograde rotation has the obvious advantage that the frequency of the tide seen from the rest frame of the B-star is considerably higher than for prograde rotation, causing excitation of very low order g-modes to large amplitudes. However, the dissipation times for low order g-modes, which set the rate at which orbital energy is extracted by the star, are considerably longer than the dissipation times of the higher order g-modes excited in a non-rotating star. This offsets the advantage of having increased mode amplitudes in a retrograde rotating star. For a concise and physically motivated derivation of this result please see Kumar & Quataert (1996).

In the next section we describe the orbital evolution caused by the radiative damping of the dynamical tide in a uniformly rotating star, and discuss the probability that mode resonances may substantially speed up the rate of orbital evolution. In §3 we consider several alternate dissipation mechanisms, in particular nonlinear parametric instability (Kumar & Goodman 1996) and enhanced radiative dissipation in a differentially rotating star, in order to assess if they might be important for understanding the orbital evolution of the PSR J0045-7319 Binary. Please note that all frequencies in this paper, including rotational and orbital angular speeds, are given in micro-Hz (μHz) unless explicitly stated otherwise.

§2 Dynamical tide in a uniformly rotating star

Consider a binary system where the primary star has mass M_* , and its companion, the secondary star, has mass M . The primary is assumed to be rotating as a solid body with the component of its angular velocity normal to the orbital plane of Ω_* .

The tidal forcing of a star predominantly excites gravity modes (g-modes) since they have periods comparable to the period of the tidal forcing. The g-modes in a uniformly rotating star are specified uniquely by three numbers: n the number of radial nodes, λ , which is in general not an integer, is a generalization of the spherical harmonic degree ℓ , and m , the azimuthal order.¹ The mode amplitude in the rotating reference frame of the star, $A_\alpha^{(r)}$ (α denotes the collective index n, λ, m), for the dominant quadrupole tide, can be calculated by decomposing the tidal forcing function in terms of its Fourier coefficients and is given below (see Kumar et al. 1995, and Quataert et al. 1996 for details)

$$A_\alpha^{(r)}(t) \approx f_\alpha \exp(im\Omega_* t) \sum_{k=1}^{\infty} \frac{D_k^{(2m)} \exp[\mp ik\Omega_0 t \mp i\phi_k]}{\sqrt{[r_\alpha^2 - (k - |m|s)^2]^2 + d_\alpha^2 (k - |m|s)^2}} \quad (1)$$

where

$$f_\alpha = \frac{4\pi}{5} \frac{GM\omega_\alpha^2 Q_\alpha}{a^3}, \quad r_\alpha = \frac{\omega_\alpha}{\Omega_o}, \quad d_\alpha = \frac{\Gamma_\alpha}{\Omega_o}, \quad s = \frac{\Omega_*}{\Omega_o}, \quad \tan \phi_k = \frac{d_\alpha (|m|s - k)}{r_\alpha^2 - (k - |m|s)^2}, \quad (2)$$

$\Omega_o = \sqrt{G(M + M_*)/a^3}$ is the orbital frequency, a is the semi-major axis of the orbit, $D_k^{(2m)}$ are the fourier coefficients of the quadrupole tidal forcing function, Γ_α is the mode's energy dissipation rate, and Q_α is the overlap of the mode's normalized Eulerian density perturbation, $\delta\rho_\alpha$, with the quadrupole tidal potential. The negative sign in the exponent of equation (1) is considered when m is positive.

We normalize our mode eigenfunctions so that the mode energy is equal to the square of the mode amplitude. Thus, the energy in mode α due to tidal forcing, as seen by an observer corotating with the star, is obtained by taking the square of the resonant term in the Fourier series, *i.e.*,

$$E_\alpha^{(r)} \approx \frac{f_\alpha^2 \left| D_{k_\alpha}^{(\ell m)} \right|^2}{[r_\alpha^2 - (k_\alpha - |m|s)^2]^2 + d_\alpha^2 (k_\alpha - |m|s)^2}, \quad (3)$$

where k_α is a positive integer that minimizes the denominator, *i.e.*, $k_\alpha = \lfloor s|m| \pm r_\alpha \rfloor$, where $\lfloor x \rfloor$ denotes the nearest integer to x . The net energy in the dynamical tide is $E_{tide}^{(r)} = \sum_\alpha E_\alpha^{(r)}$.

It is easy to obtain $D_k^{(2m)}$ numerically, and, for $m = \pm 2$, it peaks at $k \approx 2\Omega_p/\Omega_o$, where $\Omega_p = (1-e)^{-3/2}(1+e)^{1/2}\Omega_o$ is the orbital angular speed of the star at periastron and

¹ Because the modification to the mode structure in the rotating star is not central to our analysis, we have relegated a discussion of it to Appendix B; in addition, we often use ℓ in place of λ .

e is the orbital eccentricity. The peak value of $D_k^{(22)}$ is $\approx (1+e)^{-1} \sqrt{15/128\pi} (\Omega_p/\Omega_o)$ while for $k \gtrsim 5\Omega_p/\Omega_o$, $D_k^{(22)} \approx \exp(-1.3k\Omega_o/\Omega_p)/(1-e)^{3/2}$. The $m = 0$ Fourier coefficients, $D_k^{(20)}$, are roughly constant for k up to $2\Omega_p/\Omega_o$ and decrease exponentially at larger k . Moreover, the $D_k^{(20)}$ are typically smaller than the $D_k^{(2\pm 2)}$ by a factor of at least a few and so most of the tidal energy resides in the $m = \pm 2$ modes unless $\Omega_* \approx \Omega_p$. The peak of $D_k^{(22)}$ at $k \approx 2\Omega_p/\Omega_o$ and the exponential fall off at higher harmonics implies that the mode with the largest energy has a frequency $\omega_\alpha \approx \Omega_{tide}$ (measured in a frame corotating with the star), where $\Omega_{tide} \equiv 2|\Omega_p - \Omega_*|$ is twice the angular speed of the secondary at periastron, as seen in the rotating reference frame of the B-star. Higher frequency modes, while they have larger Q_α , have less energy because $A_\alpha^{(r)}$ decreases exponentially for larger frequencies. Lower frequency modes have less energy because they have a larger number of radial nodes and thus smaller Q_α .

The effect of stellar rotation, for $0 < \Omega_* < \Omega_p$, is to decrease the energy in modes since the resonance is shifted to higher harmonics. The modes that are most efficiently excited have $\omega_\alpha \approx \Omega_{tide}$, and so $E_{tide}^{(r)}$ decreases with increasing Ω_* as lower frequency g-modes with smaller wavelengths and smaller Q_α are excited. For $\Omega_* \approx \Omega_p$ or $\Omega_{tide} \approx 0$, the energy in the dynamical tide reaches its minimum value.²

For $\Omega_* > \Omega_p$, however, Ω_{tide} increases with increasing Ω_* , higher frequency modes are excited by the tidal forcing and so $E_{tide}^{(r)}$ increases. It is also clear from equation (3) that for retrograde rotation ($\Omega_* < 0$) the tidal frequency is larger and the energy in the dynamical tide is greater (as was pointed out by Lai, 1996). All of these effects are clearly seen in Figure (1a), which is a plot of $E_{tide}^{(r)}$, the sum of the energy in all modes (including $m = 0$ & $m = \pm 2$), as seen by an observer corotating with the B-star, for the SMC binary system as a function of the B-star's rotation rate.

The energy in a mode is proportional to δr_α^{-2} , where $\delta r_\alpha \equiv r_\alpha - |k_\alpha - |m||s|$ (see eq. [3]) and so close resonances can significantly enhance the energy in the dynamical tide. The effect of resonances is evident in Figure (1).

The mode energy as seen by an observer corotating with the star, $E_\alpha^{(r)}$, does not include the work done by the tidal force on the velocity field associated with the rotation of the star, which changes the star's rotational energy. The mode energy as seen by an inertial observer includes this contribution and is given by $E_\alpha^{(i)} = E_\alpha^{(r)} + \Omega_* L_\alpha$, where L_α , the angular momentum associated with a gravity wave of frequency ω_α and azimuthal order m can be shown to be equal to $-mE_\alpha/\omega_\alpha$. We note that E_α and ω_α are frame dependent quantities, but the ratio $E_\alpha/\omega_\alpha \propto L_\alpha$ is frame independent. The net tidal energy as seen by an inertial observer, $E_{tide}^{(i)} = \sum_\alpha E_\alpha^{(i)}$, is shown in Figure (1b) for the SMC binary system (we note that the results presented in fig. 1 were calculated using the

² This corresponds to the $m = 0$ and $m = \pm 2$ modes being excited to comparable amplitudes. For $\Omega_{tide} \neq 0$, the $m = \pm 2$ modes are excited to greater amplitudes than the $m = 0$ modes.

entire fourier series expansion of $E_{tide}^{(i)}$ and $E_{tide}^{(r)}$, rather than just the resonant term; see Appendix A).

Since (for $m \neq 0$) the azimuthal propagation of tidally excited waves, as seen by an inertial observer, is always in the direction of the orbital motion, the sign of m/ω_α is negative and is independent of Ω_* . This implies that L_α and $E_\alpha^{(i)}$ have the same sign. Since the angular momentum deposited in the star is positive for $\Omega_* \lesssim \Omega_p$, the tidal energy deposited in the star is also positive, which leads to a decrease in the orbital period with time. For $\Omega_* \gtrsim \Omega_p$, on the other hand, the sign of the angular momentum deposited reverses and so there is a net transfer of energy from the star to the orbit. Physically, for $\Omega_* \gtrsim \Omega_p$, the energy taken out of the spin of the star (which is being slowed down) exceeds the energy deposited in modes and so the orbital energy and period of the binary system increase with time. A more detailed discussion of these results is given in Appendix A.

In order to calculate the orbital evolution we need to know the dissipation rate of the dynamical tide, which we calculate in the next section.

2a. Radiative damping of g-modes

The radiative damping times for the low order quadrupole g-modes of a $8.8 M_\odot$, slightly evolved, main sequence star are given in Table 2 (the model was kindly provided by the Yale group). The dissipation was calculated by solving the fully non-adiabatic oscillation equations (see Unno et al. 1989 or Kumar 1994 for details). For $n \gtrsim 4$, the mode dissipation time decreases rapidly with increasing mode order (decreasing frequency), roughly as $\omega^{-7.5}$. This scaling is explained below using a WKB analysis.

The local radiative dissipation rate for the energy of a g-mode is (Unno et al. 1989)

$$\gamma(r) \approx \frac{\Delta T}{\epsilon(r)T} \frac{\partial \Delta F_R}{\partial r}, \quad (4)$$

where Δ denotes a Lagrangian perturbation, T and F_R are the temperature and radiative flux, respectively, and $\epsilon(r)$ is the mode's local energy density. Away from the turning points, this expression reduces to

$$\gamma(r) \approx \frac{F_R k_r^2}{\rho c_s^2 d \ln T / dr} \left(\frac{\partial \ln T}{\partial \ln \rho} \right)_p \left(\frac{\partial \ln T}{\partial \ln \rho} \right)_s, \quad (5)$$

where

$$k_r \approx \frac{1}{\omega_\alpha} [N^2 - \omega_\alpha^2]^{1/2} [\ell(\ell+1)/r^2 - \omega_\alpha^2/c_s^2]^{1/2} \quad (6)$$

is the wave's radial wave number and c_s and N are the sound speed and Brunt-Väisälä frequency, respectively. The global radiative dissipation rate for a g mode (Γ_α) is the integral of $\gamma(r)$, weighted by $\epsilon(r)$, between the lower and upper turning points:

$$\Gamma_\alpha \approx \int_{r_l}^{r_u} dr r^2 \gamma(r) \epsilon(r), \quad (7)$$

where r_u , the outer turning point of the wave, is the radius at which $\omega_\alpha^2/c_s^2(r_u) = \ell(\ell + 1)/r_u^2$. Energy conservation implies that $r^2\epsilon(r)v_g$ is independent of r (where v_g is the radial group velocity of the wave) and so the above equation reduces to

$$\Gamma_\alpha \approx \frac{F_R \ell}{\bar{N} \omega_\alpha^2} \int_{r_l}^{r_u} dr \frac{N^3 H}{r^2 \rho c_s^2} \left[\frac{\ell(\ell + 1)}{r^2} - \frac{\omega_\alpha^2}{c_s^2} \right]^{1/2}, \quad (8)$$

where $\bar{N} \equiv \int_{r_l}^{r_u} dr N/r$ is the mean value of the Brunt-Väisälä frequency. Most of the contribution to the wave damping comes from a region near the upper turning point close to the surface of the star, which moves outward with decreasing frequency. Performing this integration for a polytrope of index 2 (a value appropriate for the outer envelope of the Yale group's B-star model we are using), we find that Γ_α for g-modes scales as ω^{-7} or n^7 (and also as ℓ^7). We note that for a fixed n , the value of Γ_α for a quadrupole mode is independent of Ω_* , ω_α , and m for a uniformly rotating star (which is why we have used ℓ instead of λ in the above equations).

2b. Standard dynamical tidal evolution for the PSR J0045-7319 Binary

The rate of change of the orbital period for the SMC Binary can be calculated using the following equation

$$\frac{\dot{P}_{orb}}{P_{orb}} = -\frac{3\dot{E}_{orb}}{2E_{orb}} = \frac{3}{2E_{orb}} \sum_\alpha \Gamma_\alpha E_\alpha^{(i)} \approx \frac{3}{2E_{orb}} \sum_\alpha \frac{\Gamma_\alpha E_\alpha^{(r)} \omega_\alpha^{(i)}}{\omega_\alpha^{(i)} - m\Omega_*}, \quad (9)$$

where $\omega_\alpha^{(i)}$ is the mode frequency in an inertial frame; the frequency in the rotating frame of the star is $\omega_\alpha^{(r)} = \omega_\alpha^{(i)} - m\Omega_*$. The last equality in equation (9) follows from using the relation derived earlier between the mode energy in an inertial and rotating reference frame. The mode energy in the rotating frame of the star, $E_\alpha^{(r)}$, can be calculated using equation (3). The eigenfrequencies and the overlap of the modes with the tidal potential (Q_α) are calculated using a $10 M_\odot$ B-star model of 5.3 solar radii (provided by the Yale group). The effect of the rotation of the B-star on the mode properties is included using the 'traditional approximation' (Bildsten et al. 1996; Chapman & Lindzen 1970; Unno et al. 1989; see Appendix B for details). The mass and the radius of the B-star are observationally estimated to be about $8.8M_\odot$ and $6R_\odot$, respectively³ (Bell et al. 1995) and

³ This radius is slightly smaller than that used by Lai (who took $R_* \approx 6.4R_\odot$), and so our tidal energies are smaller than his. It can be shown that the energy in the dynamical tide scales as $E_{tide}^{(i)} \propto Q_\alpha^2 \omega_\alpha^2$ (see eq. [3]), where α is the mode that carries most of the tidal energy; the frequency of this mode in an inertial frame is $\approx 2\Omega_p$. Thus $E_{tide}^{(i)} \propto Q_\alpha^2 \approx (R_*^5/G)(n_\alpha + 1)^{-2\beta}$, where β is equal to 1.5 (3) for a polytropic star of index 3 (2), and n_α is the number of radial nodes for the g-mode with the most energy. Since $(n_\alpha + 1) \propto (2\Omega_p)^{-1} \sqrt{GM_*/R_*^3}$, we find that $E_{tide}^{(i)} \propto R_*^{3\beta+5}/M_*^\beta$; thus for stars of polytropic index 3 (2) the tidal energy increases with the stellar radius (for fixed stellar mass) as $R_*^{9.5}$ (R_*^{14}); we have verified this dependence using numerical calculations.

so we multiply the mode frequencies and overlap integrals calculated using the Yale model by a factor of 0.78 and 1.36, respectively, to account for the difference between the stellar model and the observational parameters; note that $Q_\alpha \propto R_*^{2.5}$ and $\omega_\alpha \propto (M_*/R_*^3)^{1/2}$. We have neglected the modification to the equilibrium structure of the star due to rotation in our calculations, which is likely to be a poor approximation since $\hat{\Omega}_*$ for the SMC B-star is not much smaller than one.

Figure (2) shows $\Delta E_{orb} \equiv P_{orb}\dot{E}_{orb}$ and P_{orb}/\dot{P}_{orb} for the SMC Binary as a function of the Bstar's rotation rate, $\hat{\Omega}_*$; modes of $m = \pm 2$ as well as $m = 0$ are included in these calculations.⁴ The results presented in this figure, as well as fig. 1, were obtained by artificially setting $d_\alpha = 0.2$ in the calculation of the mode amplitude, thus limiting the strength of resonances; we will subsequently discuss the probability that closer resonances significantly enhance the energy in modes and thus decrease the orbital evolution timescale. The minima of $E_{tide}^{(i)}$, $E_{tide}^{(r)}$ and ΔE_{orb} (and thus the maxima of P_{orb}/\dot{P}_{orb}) in Figures (1) and (2) correspond to the 'off-resonance' dynamical tide. They are equivalent to the calculation of the work done on the star in the absence of any oscillations, i.e., the result obtained by Press & Teukolsky 1975 (see also Lai 1996).

For $\hat{\Omega}_* < 0$ the tidal frequency is larger than for prograde rotation, and so the frequencies of the modes with the most energy are higher and their n value is lower. Thus the dissipation time of the dynamical tide is longer for retrograde rotation than for prograde rotation. For example, for $\hat{\Omega}_* \approx -0.3$, the modes with the most energy are the g_1 - g_3 modes, while for $\hat{\Omega}_* \approx 0$, the modes with the most energy are the g_4 - g_8 modes. The dissipation times are longer in the former case by a factor of about 100 (see Table 2). This is why, although the energy in the dynamical tide is about 100 times larger for retrograde rotation than for no rotation (fig. 1), the energy dissipated, and thus the orbital evolution time, is comparable in the two cases. We note that $\Omega_p/2\pi \sim 3.6\mu\text{Hz}$, which accounts for the minimum in ΔE_{orb} and the maximum in P_{orb}/\dot{P}_{orb} at $\hat{\Omega}_* \approx 0.2$ (see fig. 2), since this is where $\Omega_{tide} \approx 0$. We would also like to point out that the energy in the dynamical tide for $\hat{\Omega}_* \approx 0$ is a few times 10^{40} erg (fig. 1). If this energy is dissipated in an orbital period, the resulting orbital period evolution time is about 10^6 years, which is close to the observed value.

The observations of spin-orbit coupling in the timing data of PSR J0045-7319 provides evidence that the magnitude of the B-star's rotation rate is probably super-synchronous, that is, $|\Omega_*| \gtrsim \Omega_p$ (Lai et al. 1995; Kaspi et al. 1996). Prograde rotation at $\Omega_* \gtrsim \Omega_p$ would lead to a transfer of energy from the spin of the B-star to the orbit, causing the orbital period to increase with time (see fig. 2 and the last part of the discussion following eq. [3]), which is inconsistent with the observations; prograde super-synchronous rotation of the B-star is thus ruled out. For $\Omega_* \sim \Omega_p$ (which is consistent with the apsidal motion

⁴ We note that the results presented in Figures 1 & 2 were calculated using slightly more accurate expressions for $E_\alpha^{(i)}$ and $E_\alpha^{(r)}$ in which the entire fourier series, not just the resonant term, is kept (see Appendix A).

of the binary system) the energy in the dynamical tide is too small by about two orders of magnitude to explain the observed orbital evolution time, even if we assume that all of the tidal energy is dissipated in one orbit. These considerations force us to conclude that the rotation of the B-star must be retrograde. This is discussed further in §3.

Our calculations indicate that the orbital evolution time due to the radiative dissipation of the ‘off-resonance’ dynamical tide is at least three orders of magnitude too small to account for the observed P_{orb}/\dot{P}_{orb} of the PSR J0045-7319 binary, regardless of the B-star’s rotation rate. Is it possible, however, that the observed orbital decay rate of the PSR J0045-7319 Binary is because a low to moderate order g mode is highly resonant with the orbit ($\delta r_\alpha \approx 10^{-2}$), thus increasing the energy in the dynamical tide by about three orders of magnitude and decreasing the orbital evolution timescale to about 5×10^5 years? We think that this is highly unlikely. If the ‘off-resonance’ value of the energy in the dynamical tide is E_{or} , then the probability that we are observing the system at a time when the energy in the dynamical tide is E is $P(E) \approx N(E_{or}/E)^{3/2}$, where N is the number of low to moderate order g modes which can be resonant with the orbit. This follows from comparing the time it takes the resonant mode to move off resonance with the time it takes the orbit to evolve between resonances. From Figures (1) and (2), $E/E_{or} \approx 10^3$ in order to explain the observations and thus the probability that the orbital decay of the PSR J0045-7319 Binary is due to a resonant g mode is $\sim 0.01\%$. This probability is nearly the same for $\hat{\Omega}_* = -0.3, 0$. We thus conclude that it is highly unlikely that the orbital decay of the PSR J0045-7319 Binary is due to the radiative dissipation of the dynamical tide in a uniformly rotating star. We now consider several alternate dissipation mechanisms, including the effect of differential rotation on the damping of gravity waves.

§3. Alternative damping mechanisms for tidal waves

In the previous section we have argued that the linear radiative dissipation of the dynamical tide in a uniformly rotating B-star is incapable of explaining the observed orbital decay of the SMC Binary. The calculations of the energy in the dynamical tide are, in our opinion, relatively secure, but the understanding of dissipation mechanisms, which clearly affects our estimate of the orbital evolution time, requires closer scrutiny. Accordingly, we describe two dissipation mechanisms in this section. One of them, described below, is found to be extremely efficient in dissipating the energy of the dynamical tide when the star has some differential rotation. Another mechanism, nonlinear parametric coupling of the equilibrium tide to low frequency g-modes, is more likely to operate when the star is rigidly rotating. This is discussed in §3b.

3a. The effect of differential rotation on the radiative damping of gravity waves

The unusual (non-periodic) time residuals for the pulse arrival times of PSR J0045-7319 provides strong evidence for spin-orbit coupling in the PSR J0045-7319 Binary and suggests that the interior of the B-star is rapidly rotating with its spin axis inclined with

respect to the normal to the orbital plane (Kaspi et al. 1996; Lai et al. 1995). We can readily estimate the relative timescales for spin pseudo-synchronization and orbital circularization for the SMC system to see if the B-star should, from a theoretical point of view, be rotating pseudo-synchronously (i.e., with $\Omega_* \approx \Omega_p$).⁵

The rate of change of the stellar rotation due to the transfer of orbital angular momentum to the star is $|\dot{\Omega}_*|/\Omega_* \approx (L_{orb}/L_*) (|\dot{L}_{orb}|/L_{orb})$, where $L_{orb}/L_* \approx 4\hat{\Omega}_*^{-1}$. Using $\dot{L}_{orb} = \dot{E}_{orb}/\Omega_p$ for the dynamical tide (see §2 and appendix A), as well as for the equilibrium tide⁶, we find that $|\dot{\Omega}_*|/\Omega_* \approx 0.2 \hat{\Omega}_*^{-1} (|\dot{E}_{orb}|/E_{orb})$. Thus so long as the B-star is rotating near break up ($|\hat{\Omega}_*| \gtrsim 0.2$), *both* the equilibrium and the dynamical tides lead to timescales for spin pseudo-synchronization which are comparable to the orbital circularization time. We therefore do not expect that the rotation rate in the interior of the B-star has changed appreciably, which is consistent with the observations.

We do expect, however, that the dynamical tide should have forced the surface layers of the B-star into pseudo-synchronous rotation. The physical reason for this follows from the seminal work of Goldreich and Nicholson (1989), who showed that tidal waves deposit their angular momentum at the place in the star where they are dissipated. Since the dissipation rate is largest near the surface of the star (see §2b) and the moment of inertia of the surface region is a small fraction of the star's total moment of inertia, the surface of the star tends to be pseudo-synchronized very rapidly. For the SMC binary system with a rapidly retrograde rotating B-star ($\hat{\Omega}_* \approx -0.3$), the modes with the most energy have frequencies $\approx 17\mu\text{Hz}$ in the rotating reference frame. Figure (3) shows $\gamma(r)$, the local radiative dissipation rate, for such a mode. The dissipation is concentrated in a layer $\approx 0.05R_*$ thick near the outer turning point, which occurs at $r \approx 0.85R_*$. The moment of inertia of this layer is $\approx 10^3$ times smaller than that of the entire star and so we expect the rotation of the B-star at $r \approx 0.85R_*$ to be pseudo-synchronous. The dominant tidal waves are, however, evanescent at $r \gtrsim 0.85R_*$, and lower frequency waves with outer turning points near the surface of the star ($\omega_\alpha/2\pi \lesssim 5\mu\text{Hz}$) carry insufficient angular momentum to bring the surface ($r \gtrsim 0.85R_*$) into pseudo-synchronous rotation. The large positive entropy gradient in the radiative exterior of the B-star (the Brunt-Väisälä frequency is $\approx 70\mu\text{Hz}$) has a strong stabilizing effect on shear instabilities which could otherwise retard the surface rotation and reduce the differential rotation of the region at $r \approx 0.85R_*$. Therefore, provided that magnetic stresses do not efficiently transport angular momentum between the stellar surface and the pseudo-synchronous layer, the rotation rate of the B-star at $r \gtrsim 0.85R_*$ is expected to be approximately the same as it was at the initial time. The optical linewidth measurement of Bell et al. (1995) gives a surface rotation

⁵ The relative timescale calculation is significantly more secure than a calculation of the absolute timescale for pseudo-synchronization since it depends only on the ratio of the energy to the angular momentum in the tide.

⁶ The equilibrium tide in the weak friction limit is discussed in detail in the seminal paper of Hut (1981), who also finds $\dot{E}_{orb} \approx \Omega_p \dot{L}_{orb}$.

frequency of $\approx 4/\sin(i_{ns}) \mu\text{Hz}$, where i_{ns} is the angle between the spin axis and the line of sight. If correct, this suggests that the observed surface of the star is perhaps not pseudo-synchronized. In what follows, we shall assume that there is a region below the surface of the star that rotates close to the pseudo-synchronous value and describe how this dramatically enhances the dissipation of the dynamical tide.

We have calculated g-mode eigenfunctions in rigidly and differentially rotating stars and an example of the adiabatic energy flux for a g-mode is shown in Figure (4). The differential rotation was chosen to conform to that expected from the radiative dissipation of the dynamical tide in the B-star of the PSR J0045-7319 Binary, i.e., the thickness of the differentially rotating layer was taken to be $\approx 0.1R_*$ centered at $r \approx 0.8R_*$. We note that the energy flux is nearly constant across the differentially rotating layer, indicating that there is very little reflection of the wave at this layer; furthermore, the wavelength of the wave has decreased dramatically in the differentially rotating layer, which results in a strongly enhanced dissipation rate.

The frequency of tidally excited gravity waves, as seen by an inertial observer, is $\approx 2\Omega_p$ (see §2a). If the component of the rotation rate of the star normal to the orbital plane a distance r from the center is $\Omega_*(r)$, then the frequency of the gravity wave in the local rest frame of the fluid is $\omega_r \approx 2|\Omega_*(r) - \Omega_p|$ and its wavenumber is $\approx 6^{1/2}N(r)/(r\omega_r)$. Thus, as the wave approaches the pseudo-synchronously rotating surface of the star its wavelength goes to zero and the energy it carries is entirely dissipated.⁷ Even if the rotation of the B-Star in the SMC Binary at $r \approx 0.85R_*$ is not fully pseudo-synchronized, the dynamical tide will be completely absorbed as it approaches the surface provided that its local radiative dissipation rate becomes comparable to the wave frequency. We find that this occurs so long as the frequency of the gravity wave in the local rest frame of the star near $r \approx 0.85R_*$ is less than about $2\mu\text{Hz}$, which requires that the stellar rotation frequency at $r \approx 0.85R_*$ be within about $1\mu\text{Hz}$ (or 30%) of its pseudo-synchronous value. This requirement, which is not particularly stringent, is weakened further if waves can travel closer to the surface of the star, such as when there is redistribution of angular momentum due to internal stresses in the outer envelope of the star.

Let us assume that the energy input into the waves, inspite of the enhanced dissipation, is approximately equal to the energy in tidal oscillations calculated in §2a in the absence of resonances (the error due to this assumption is discussed below). From Figure 1 we see that this energy input is $\approx 2 \times 10^{41}$ ergs per orbit when the star is rotating with $\hat{\Omega}_* = -0.3$ ($\Omega_*/2\pi \approx -6\mu\text{Hz}$). Using $P_{orb}/\dot{P}_{orb} = -2E_{orb}/3\dot{E}_{orb}$ with an energy loss

⁷ As the wave frequency goes to zero, the effect of the Coriolis force on the wavefunction becomes increasingly important and it might appear that this will adversely affect the dissipation of the wave. Using the ‘traditional approximation’ (Appendix B), however, it can be shown that, for a fixed wave frequency and a surface rotation rate which is slightly sub-synchronous, including the Coriolis force tends to increase the wavelength of the wave by only $\approx 20\%$, and thus the dissipation of the wave remains essentially the same.

per orbit of $\Delta E_{orb} \approx E_{tide}^{(i)} \approx 2 \times 10^{41}$ ergs, we find an orbital period evolution time for the SMC binary of $\approx 10^5$ years, which is a factor of about 5 smaller than the observed timescale.

Thusfar we have ignored the modification to the g-mode eigenfunction in the differentially rotating star. As Figure (4) shows, in the outer part of the star where the stellar rotation rate approaches its pseudo-synchronous value, the wavelength of the gravity wave becomes very small. Thus, the coupling of gravity waves to the tidal forcing function is reduced, i.e., there is very little contribution to the overlap integral from the outer part of the star ($r \gtrsim 0.8R_*$). The exact amount by which the overlap integral is reduced in the differentially rotating star depends on the details of the differential rotation and the modes which are excited, and is somewhat uncertain.⁸ Our estimates suggest that for the very low order modes excited in the rapidly retrograde rotating B-star, Q_α decreases by a factor ~ 2 due to the differential rotation and so the energy in the dynamical tide decreases by about a factor ~ 4 . This increases our estimate of the orbital period evolution timescale of the PSR J0045-7319 Binary to $\approx 4 \times 10^5$ years, which is consistent with the observations. In fact the theoretically calculated orbital evolution times are consistent with the observations so long as $0.3 \lesssim \hat{\Omega}_* \lesssim 0$.

We note that prograde rotation of the B-star at $\hat{\Omega}_* \approx 0.4$ gives an orbital evolution time of comparable magnitude, though with the opposite sign. Thus our reason for suggesting retrograde rotation is not to explain the short timescale for orbital evolution (which prograde rotation can also do), but rather to insure that the tidal interactions result in a decrease in the orbital period with time, as is found by the observations. For $\hat{\Omega}_* \sim 0.1$ (which is roughly the observational lower limit obtained from the apsidal motion of the system, cf. Kaspi et al. 1996) the energy in the dynamical tide is less than a few times 10^{39} erg; the resulting orbital evolution time, assuming that all of this energy is dissipated in one orbit, is greater than about 3×10^7 years, which is a factor of ≈ 50 larger than the observed value. For $\hat{\Omega}_* \approx 0$, on the other hand, the energy in the tide is about 2×10^{40} erg and thus the orbital period is expected to decrease on a time scale of $\sim 10^6$ years. This small rotation rate is, however, inconsistent with the observed apsidal motion of the system (Kaspi et al. 1996), which is why we are forced to consider retrograde rotation.

It is straightforward to show that the rate of change of the orbital eccentricity is given by $\dot{e} \approx [(1 - e^2)/3e](\dot{P}_{orb}/P_{orb})$. Thus we expect $\dot{e}^{-1} \approx 3 \times 10^6$ years, which is a factor of about 20 larger than the current lower limit of Kaspi et al. (1996).

⁸ When the tidal frequency is much less than quadrupole f-mode frequency, almost all of the forcing by the tidal potential occurs near the interface of the convective core and the radiative exterior where the wavelength of the wave is the longest. Thus, differential rotation in the outer part of the star would not substantially modify the coupling of the wave to the tidal force. This limit is, however, not applicable to the very low order modes excited in the rapidly retrograde rotating B-star.

If magnetic stresses and/or instabilities are very efficient in redistributing angular momentum in the B-star so that, inspite of the tidally excited waves depositing angular momentum at $r \sim 0.85R_*$, the star continues to rotate almost rigidly, the dissipation of gravity waves will not be enhanced as described above. However, tides may still be efficiently dissipated by the nonlinear process discussed by Kumar and Goodman (1996). This is considered in some detail below.

3b. Parametric coupling of the dynamical and equilibrium tides with g-modes

When a primary mode, denoted by α and taken to be either the dynamical or the equilibrium tide, drives a mode of half its frequency (referred to as the daughter mode and denoted by β) by nonlinear mode coupling, the process is called parametric instability. This process was proposed by Kumar & Goodman (1996) for damping the dynamical tide in late type stars, and was found to be much more efficient than conventional turbulent and/or radiative dissipation for close binary systems. We consider this process for the B-star of the SMC binary.

The growth rate of the energy of the daughter mode, subject to parametric driving, is given by (Kumar & Goodman, 1996)

$$\eta = \left[\sqrt{18E\kappa_{\alpha\beta\beta}^2\omega_\beta^2 - (\Delta\omega)^2} - \frac{\Gamma_\beta}{2} \right], \quad (10)$$

where E is the energy in the primary mode, $\Delta\omega \equiv \omega_\alpha - 2\omega_\beta$, Γ_β is the linear energy dissipation rate of the daughter mode, and $\kappa_{\alpha\beta\beta}$ is the nonlinear 3-mode coupling coefficient (the calculation of which is somewhat involved and is described in Kumar & Goodman). Thus, parametric instability sets in only if there are modes in the star which can simultaneously satisfy:

$$|\Delta\omega| < 3\sqrt{2}E^{1/2}\kappa_{\alpha\beta\beta}\omega_\beta \quad (11)$$

and

$$\Gamma_\beta < 6\sqrt{2}E^{1/2}\kappa_{\alpha\beta\beta}\omega_\beta. \quad (12)$$

These two conditions compete in the sense that higher ℓ g-modes have smaller frequency spacings and are thus more likely to satisfy equation (11), but they have larger dissipation rates and are thus less likely to satisfy equation (12).

The damping rate, Γ_β , for g-modes of early type stars increases as ℓ^7 (see §2a), and so only low ℓ daughter modes can satisfy equation (12). For retrograde rotation of $\hat{\Omega}_* = -0.3$, the energy in the primary modes ($g_2 - g_4$) is $E \approx 2 \times 10^{41}$ ergs (see Fig. 1), and the 3-mode coupling coefficient of these modes with daughters of half their frequency is $\kappa_{\alpha\beta\beta} \approx 10^{-25} \text{ erg}^{-1/2}$. Thus, we must find a daughter mode with $|\Delta\omega|/\omega_\beta \approx 10^{-4}$ and $\Gamma_\beta \lesssim 3 \times 10^{-8} \text{ s}^{-1}$ in order for the dynamical tide to be parametrically unstable. The small damping time required for the daughter modes implies that it must be of degree less than ~ 3 . However, since the g-mode frequencies in the B-star of the SMC binary are

$\sim (n+1)^{-1} \sqrt{\ell(\ell+1)} 27 \mu\text{Hz}$, it is very unlikely (the probability is less than $\approx 0.1\%$) that there is such a low degree daughter mode with a frequency within the required tolerance that can couple to the primary mode. We thus conclude that the dynamical tide in the PSR J0045-7319 Binary is stable against parametric instability. We show below, however, that the equilibrium tide is subject to the parametric instability.

The equilibrium tide represents the hydrostatic response of the primary to the perturbing gravitational force of the secondary. The structure of the equilibrium tidal perturbation is similar to that of the f mode. The frequency of the equilibrium tide, $\Omega_{tide} = 2|\Omega_p - \Omega_*|$, is, however, much smaller than that of the f mode. Thus the nonlinear coupling of the equilibrium tide to its daughter modes is analogous to the coupling of the f mode to very low frequency ($\omega_\beta \approx \Omega_{tide} \ll \omega_f$) daughter modes, rather than to daughter's of half its frequency, as was the case for the dynamical tide. For $\omega_\beta \ll \omega_f$, it can be shown that the coupling coefficient is proportional to the square of the daughter's normalized transverse displacement eigenfunction, which is proportional to ω_β^{-2} . Thus, the coupling coefficient for the equilibrium tide is significantly larger than for the dynamical tide. For $\ell \approx 1$ daughter modes, $\kappa_{\alpha\beta\beta} \approx 4 \times 10^{-22} \nu_\beta^{-2} \text{erg}^{-1/2}$, where $\nu_\beta = \omega_\beta/2\pi$ is the daughter mode frequency in micro-Hz.⁹

The energy in the equilibrium tide near periastron is $E_{eq} \approx k(R_*/R_{peri})^6 GM^2/R_* \sim 10^{42}$ ergs, where $R_{peri} \approx 4R_*$ is the separation between the two stars at periastron and $k \sim 0.008$ is the apsidal motion constant of the B-star. The energy in the equilibrium tide falls off rapidly from periastron, so parametric instability can only set in and daughter modes can only grow near periastron. We thus define an orbit averaged growth rate for a daughter mode as $\bar{\eta} \equiv \eta\Omega_o/\Omega_p$, where η is calculated using the energy in the equilibrium tide at periastron. If $\bar{\eta} > \Gamma_\beta$, the daughter mode has net growth over an orbit.

For rapid prograde rotation of the B-star ($\Omega_* > \Omega_p$) the dissipation of the equilibrium tide causes the orbital period to increase with time, as was the case with the dynamical tide discussed in §2 (see appendix A and Hut 1981 for a detailed discussion). Thus, only nonlinear dissipation of the equilibrium tide in a rapidly retrograde rotating B-star can potentially explain the observed orbital period decrease of the SMC binary.

For the SMC binary system, using the values given above for E_{eq} and $\kappa_{\alpha\beta\beta}$ (and taking $\nu_\beta \approx 8\mu\text{Hz}$, appropriate for retrograde rotation at $\hat{\Omega}_* \approx -0.3$) we estimate that $\eta \approx 10^{-6} \text{s}^{-1}$ and $\bar{\eta} \approx 10^{-7} \text{s}^{-1}$. Thus we need to find daughter modes within about 0.2 μHz of 8 μHz which is possible for $\ell_\beta \geq 2$ when we consider the lifting of m-degeneracy by stellar rotation. We also find that $\bar{\eta} > \Gamma_\beta$ so long as $\ell_\beta \lesssim 4$ (using $\Gamma_\beta \propto \ell_\beta^7$ and the damping of quadrupole modes given in Table 2). Thus, we conclude that the equilibrium tide in the SMC Binary is subject to parametric instability which, as we see below, results

⁹ For $\nu_\beta = 30\mu\text{Hz}$ (half the f mode frequency), this gives $\kappa_{\alpha\beta\beta} \approx 10^{-25} \text{erg}^{-1/2}$, which agrees well with the nonlinear coupling of the low order dynamical tide given above, as is expected since the equilibrium tidal perturbation is similar to that of the f mode.

in a rather efficient dissipation of its energy.

The mean growth time of these daughter modes is $\bar{\eta}^{-1} \approx 100$ days. The resulting nonlinear dissipation time for the equilibrium tide (t_{nl}) depends on the energy in the daughter modes, which is expected to be comparable to the energy in the equilibrium tide since the daughter modes are not likely to lose energy to granddaughter modes via parametric instability. Thus, $t_{nl} \approx \eta^{-1}$. The orbital evolution timescale which results from the nonlinear dissipation of the equilibrium tide is $P_{orb}/\dot{P}_{orb} \approx (E_{orb}/E_{eq}) (\Omega_p/\Omega_o) t_{nl} \sim \bar{\eta}^{-1} (E_{orb}/E_{eq}) \sim 10^5$ years, in reasonable agreement with the observations.

We feel, however, that the case for nonlinear damping in the SMC Binary, while encouraging, is not entirely robust. This is because the nonlinear growth rate of the daughter modes is comparable to their linear radiative damping rates and because there are not many daughter modes available for coupling with the equilibrium tide. Thus a change by a factor of a few in either $\kappa_{\alpha\beta}$ or Γ_β , which is within the uncertainty of the stellar model, could modify our conclusion.

4. Discussion

The PSR J0045-7319 Binary in the SMC consists of a radio pulsar in a 51 day, highly eccentric ($e=0.808$), orbit with a B-star companion of mass $\approx 8.8M_\odot$. The orbital period of this system is observed to be decreasing on timescale of $\approx 5 \times 10^5$ years (Kaspi et al. 1996), which is several orders of magnitude faster than that expected from the standard theory of the dynamical tide. Timing observations of PSR J0045-7319, as well as optical linewidth measurements, show that the B-star is rapidly rotating with a rotation speed that is perhaps greater than the orbital angular speed of the star at periastron (Lai et al. 1995, Kaspi et al. 1996, Bell et al. 1995).

We find that for rapid prograde rotation of the B-star (rotation frequency greater than the orbital angular speed of the star at periastron) the dissipation of both the equilibrium and dynamical tides lead to an increase in the orbital period of the binary system. This is because the tidal torque is slowing down the spin of the star and the resultant loss of rotational kinetic energy exceeds the energy deposited in the tide. Thus, we infer that the B-star must have retrograde rotation if tidal effects are to account for the observed period decrease of the PSR J0045-7319 Binary. Lai (1996) has suggested that rapid retrograde rotation of the B-star can explain the orbital evolution. We certainly agree with this conclusion. However, our reason for requiring retrograde rotation is entirely different from his. This point is clarified below.

We find that for $\hat{\Omega}_* \equiv \Omega_*(R_*^3/GM_*)^{1/2} = -0.3$ (0.0) the energy in the dynamical tide, as seen from an inertial frame, is about 2×10^{41} (2×10^{40}) erg and the number of radial nodes for the most excited g-mode is 3 (6).¹⁰ The much larger energy in the dynamical tide for

¹⁰ Our energies are smaller than those of Lai in part because we use different reference frames and stellar models, and also because we use a somewhat smaller stellar radius (see

rapid retrograde rotation was correctly pointed out by Lai. However, he took the damping time of g-modes to be independent of frequency (with a value of about 14 years) and concluded that the increase in the tidal energy for rapid retrograde rotation could account for the observed rapid evolution of the PSR J0045-7319 Binary. We have shown, however, that for a rigidly rotating star the mode dissipation time increases rapidly with frequency (roughly as ω^7) and so the high frequency modes excited in the retrograde rotating B-star are much less efficiently damped than the lower frequency modes excited in a non-rotating B-star. The damping time of the dynamical tide, in a rigidly rotating star, for $\hat{\Omega}_* = -0.3$ (0.0) is given in Table 2 to be about 1.1×10^3 (50) years (the dissipation was calculated by solving the fully nonadiabatic oscillation equations and the results are consistent with, for example, those of Saio & Cox 1980). Thus the orbital evolution time for rapid retrograde rotation of the B-star, inspite of the enhanced energy in the tide, is the same as for no rotation and is $\approx 10^9$ years, or a factor of 10^3 longer than the observed value. We thus emphasize that retrograde rotation of the B-star is required, not because the standard theory for the dissipation of dynamical tide in a retrograde rotating star can explain the observed period decrease of the PSR J0045-7319 Binary (as Lai suggested), but rather because rapid prograde rotation of the B-star would lead to orbital period growth, which is inconsistent with the observations. In fact, with the enhanced dissipation mechanisms discussed below, the orbital evolution timescale for $\hat{\Omega}_* \approx +0.4$ is also consistent with the observations, but of course in this case the orbital period increases with time.

The energy in the dynamical tide for $\hat{\Omega}_* \approx -0.3$ is about 10^{41} erg (fig 1b). If this energy is dissipated in about an orbital period then the resulting theoretical time scale for the evolution of the orbital period is similar to the observed orbital decay time for the SMC Binary. We have considered two different dissipation mechanisms that satisfy this property. One of these requires significant differential rotation of the B-star, which is expected when a star is not pseudo-synchronized. This is because the gravity waves deposit their angular momentum in the outer layers of the B-star where the dissipation occurs and where the moment of inertia is much smaller than in the interior (Goldreich & Nicholson 1989). For $\hat{\Omega}_* = -0.3$, the dissipation of the dynamical tide in the B-star is concentrated at $r \approx 0.85R_*$ and so, provided that magnetic torques and/or instabilities do not force this region into solid body rotation with rest of the star, this region should be rotating pseudo-synchronously (i.e., with a rotation frequency close to the orbital angular frequency of the star at periastron, $\Omega_p/2\pi \approx 3.6\mu\text{Hz}$).

The frequency of the dynamical tide in an inertial reference frame is $\approx 2\Omega_p$ and so the frequency in the local rest frame of the star is $\approx 2[\Omega_p - \Omega_*(r)]$, where $\Omega_*(r)$ is the component of the stellar rotation rate at radius r normal to the orbital plane. Thus, the frequency and wavelength of the dynamical tide in the local rest frame of the star decrease as the wave approaches the pseudo-synchronously rotating layer. The decreasing wavelength results in the entire gravity wave energy flux being dissipated by radiative diffusion near the surface

the footnote in §2b).

of the star, provided that the rotation frequency of the star at $r \approx 0.85R_*$ is within about 30% of the pseudo-synchronous value. This enhanced dissipation readily accounts for the observed orbital period decrease of the PSR J0045-7319 Binary so long as $-0.3 \lesssim \hat{\Omega}_* \lesssim 0$. The resulting timescale for the evolution of the orbital eccentricity ($1/\dot{e}$) of the PSR J0045-7319 Binary is $\approx 3 \times 10^6$ years, which is a factor of about 20 larger than the lower limit of Kaspi et al. (1996).

The observed orbital period evolution can also be understood provided that the interior of the B-star is rotating very slowly (with the exterior close to the surface rotating pseudo-synchronously).¹¹ Slow rotation of the B-star's interior ($|\hat{\Omega}_*| \lesssim 0.1$) is, however, ruled out by the apsidal motion observations of Kaspi et al. (1996). Thus retrograde rotation of the B-star with $\hat{\Omega}_*$ between ≈ -0.3 and ≈ -0.1 appears to be the only solution that fits all of the current observations of this binary system.

In the likely scenario that the binary system was synchronized and circularized prior to the supernova that created the pulsar, the current retrograde rotation of the B-star implies that the supernova had a dipole asymmetry which imparted a net angular momentum kick to the system. This point was also made by Kaspi et al. on the basis of the misalignment of the spin and angular momentum axes.

We note that in order for this mechanism to work the B-star must have a large gradient of differential rotation in the outer envelope, with the specific angular momentum decreasing outward in the star. This can lead to thermal instabilities such as the Goldreich-Schubert-Fricke instability, and it is unclear to us whether angular momentum will be mixed efficiently as a result (the star is, however, dynamically stable because of the large positive entropy gradient in the radiative exterior). This is an important issue which we have not addressed and which needs to be investigated by a careful nonlinear calculation.

Another dissipation mechanism we have considered is nonlinear parametric instability of the equilibrium tide, which can operate when the differential rotation in the star is small. In this case energy is transferred, via resonant 3-mode coupling, from the large scale perturbation associated with the equilibrium tide to low degree g-modes of half the tidal frequency; the timescale for this process is found to be $\sim 10^2$ days for the B-star of the SMC binary and the resulting orbital evolution timescale is a few hundred thousand years. The margin of instability in our calculation is, however, small and so we are not confident that this dissipation process is operating in the B-star of the SMC binary system.

Acknowledgment: We thank Dong Lai for sending us his paper prior to publication which we found helpful to our thinking about this problem. We are very grateful to Jeremy

¹¹ Figure 1b shows that the tidal energy for a slowly rotating B-star, $\hat{\Omega}_* \approx 0$, is about 10^{40} ergs, which is a factor of ~ 5 smaller than what is needed to explain the orbital evolution. The tidal energy, however, depends on the radius of the B-star, which is not precisely known; thus, if the radius of the star is some what larger than the value we have chosen, the tidal energy will be larger than the value shown in figure 1.

Goodman for numerous discussions, for sharing with us his insight on nonlinear damping of the equilibrium tide that led to §3b, and for suggesting a number of improvements to our presentation. Obviously it is not his fault if, inspite of this, there are mistakes in the paper. We also thank Vicky Kaspi for comments.

Appendix A

In this appendix we calculate the relationship between the angular momentum and energy deposited by the tidal force for the dynamical and equilibrium tides. The quadrupole tidal gravitational potential, as seen by an observer corotating with the primary star, is given by

$$U = -\beta r^2 \sum_m Y_{2m}^*(\theta, \phi) \tilde{f}_{2m}^*, \quad (A1)$$

where

$$\beta = \frac{4\pi}{5} \Omega_o^2 \frac{M}{M + M_*} \quad (A2)$$

and

$$\tilde{f}_{2m} = \frac{Y_{2m}^*(\pi/2, \phi_{orb}(t) - \Omega_* t)}{(R(t)/a)^3}. \quad (A3)$$

The torque exerted on the primary star by the tidal force is only in the \hat{z} direction (taking, for simplicity, the rotation axis to be perpendicular to the orbital plane) and is given by

$$\tau_z = - \int d^3x (\mathbf{r} \times \nabla U)_z \delta\rho, \quad (A4)$$

where $\delta\rho$, the Eulerian perturbation to the density of the star, can be expanded in normal modes as $\delta\rho = \sum_\alpha A_\alpha \delta\rho_\alpha Y_{\ell m}(\theta, \phi)$. Substituting the tidal gravitational potential (eq. [A1]) into equation (A4), we get

$$\tau_z = -i\beta \sum_\alpha m A_\alpha Q_\alpha \tilde{f}_{2m}^*. \quad (A5)$$

The non-dimensional function \tilde{f}_{2m} can be expanded in a fourier series as (Kumar et al. 1995; Quataert et al. 1996)

$$\tilde{f}_{2m} = \exp(im\Omega_* t) \left[\sum_{k=1}^{\infty} C_k^{2m} \sin(k\Omega_o t) + \sum_{k=0}^{\infty} D_k^{2m} \cos(k\Omega_o t) \right], \quad (A6)$$

where $\text{Im}(D^{20}) = C^{20} = 0$, $\text{Im}(D_k^{2\pm 2}) = \text{Re}(C_k^{2\pm 2}) = 0$, and, for $k \gtrsim$ a few, $\text{Re}(D_k^{2\pm 2}) \approx -\text{sign}(m)\text{Im}(C_k^{2\pm 2})$. Using equation (A6) one can expand the mode amplitude in a fourier series and obtain (c.f. Kumar et al. 1995)

$$A_\alpha = \frac{\beta Q_\alpha \omega_\alpha^2}{2\Omega_o^2} \exp(im\Omega_* t) \sum_k \left[(D_k^{2m} + iC_k^{2m}) \frac{\exp[-ik\Omega_o t - i\phi_k(m)]}{\eta_k(m)} + (D_k^{2m} - iC_k^{2m}) \frac{\exp[ik\Omega_o t + i\phi_k(-m)]}{\eta_k(-m)} \right] \quad (A7)$$

where $\eta_k^2(m) = [r_\alpha^2 - (k - ms)^2]^2 + d_\alpha^2(k - ms)^2$ and the other symbols are the same as defined in equation (2) of the main text. Note that A_α given above is as seen by an

observer corotating with the star. In what follows, we shall assume that $\text{Re}(D_k^{2\pm 2}) = -\text{sign}(m)\text{Im}(D_k^{2\pm 2})$ for all k . We find that this yields values for the energy and angular momentum deposited in the star which are accurate to within at least 5 %. Substituting the fourier series expansions of the mode amplitude and the tidal forcing function into the expression for the tidal torque [A5], we find that the angular momentum deposited in the star, in one orbit, is given by

$$\Delta L \equiv \int_0^{2\pi/\Omega_o} dt \tau_z = -\frac{8\pi\beta^2}{\Omega_o^2} \sum_n Q_{n22}^2 \omega_{n22}^2 d_{n22} \sum_k \frac{(D_k^{22})^2}{[\eta_k(2)]^2} (2\Omega_* - k), \quad (\text{A8})$$

where we have summed over $m = \pm 2$ in arriving at the above expression. We note that m/ω_α has the same sign for $m = \pm 2$ modes (see eq. [A7] or eq. [2] of the main text) and so the modification to ω_α and Q_α by the Coriolis force is the same for these modes (see Appendix B).

The energy input rate into the star is given by

$$\dot{E} = - \int d^3x \rho \nabla U \cdot \mathbf{v}, \quad (\text{A9})$$

where \mathbf{v} , the fluid velocity in the star, depends on the reference frame. In an inertial reference frame, $\mathbf{v}_i = \mathbf{v}_r + \boldsymbol{\Omega}_* \times \mathbf{r}$, where $\mathbf{v}_r = \sum_\alpha dA_\alpha/dt \boldsymbol{\xi}_\alpha Y_{\ell m}(\theta, \phi)$ is the fluid velocity as seen by an observer corotating with the star (and is due to the tidally excited oscillations) and $\boldsymbol{\Omega}_* \times \mathbf{r}$ is the fluid velocity due to the rotation of the star (as seen by an inertial observer). It is straightforward to show from equations (A4) and (A9) that the energy input as seen by an inertial observer, $\dot{E}_{tide}^{(i)}$, is related to the energy input as seen by an observer corotating with the star ($\dot{E}_{tide}^{(r)}$) by $\dot{E}_{tide}^{(i)} = \dot{E}_{tide}^{(r)} + \Omega_* \tau_z$. The change in the orbital energy per orbit includes both the energy input in the modes, $\dot{E}_{tide}^{(r)}$, and the changing rotational energy of the star ($\Omega_* \tau_z$) and is thus given by

$$\Delta E_{orb} = - \int_0^{2\pi/\Omega_o} dt \dot{E}_{tide}^{(i)}. \quad (\text{A10})$$

We now calculate $\dot{E}_{tide}^{(r)}$ using the fourier series

$$\dot{E}_{tide}^{(r)} = - \sum_\alpha \frac{dA_\alpha}{dt} \int d^3x U \delta\rho_\alpha Y_{\ell, m}(\theta, \phi) = \beta \sum_\alpha \frac{dA_\alpha}{dt} Q_\alpha \tilde{f}_{2m}^*. \quad (\text{A11})$$

Substituting equations [A6] & [A7] into the above equation we obtain

$$\begin{aligned} \Delta E_{tide}^{(r)} \equiv \int_0^{2\pi/\Omega_o} dt \dot{E}_{tide}^{(r)} &= \frac{4\pi\beta^2}{\Omega_o^4} \sum_n Q_{n22}^2 \omega_{n22}^2 d_{n22} \sum_k \frac{(D_k^{22})^2}{[\eta_k(2)]^2} (2\Omega_* - k)^2 \\ &+ \frac{\pi\beta^2}{\Omega_o^4} \sum_n Q_{n20}^2 \omega_{n20}^2 d_{n20} \sum_k \frac{(D_k^{20})^2}{[\eta_k(0)]^2} k^2, \end{aligned} \quad (\text{A12})$$

where the first term in the above expression is due to the contribution of $m = \pm 2$ modes and the second (which is generally small compared to the first) is due to the $m = 0$ modes. Note that the tidal energy as seen by an observer corotating with the star is positive definite (see Figure 1). The change in the orbital energy per orbit, $\Delta E_{orb} = -\Delta E_{tide}^{(i)} = -(\Delta E_{tide}^{(r)} + \Omega_* \Delta L)$, is given by

$$\begin{aligned} \Delta E_{orb} = & \frac{4\pi\beta^2}{\Omega_o^4} \sum_n Q_{n22}^2 \omega_{n22}^2 d_{n22} \sum_k \frac{(D_k^{22})^2}{[\eta_k(2)]^2} k(2\Omega_* - k) \\ & - \frac{\pi\beta^2}{\Omega_o^4} \sum_n Q_{n20}^2 \omega_{n20}^2 d_{n20} \sum_k \frac{(D_k^{20})^2}{[\eta_k(0)]^2} k^2 \end{aligned} \quad (A13)$$

For the results presented in this paper (e.g., Figures 1 & 2), we have used the full fourier series expression for E_{tide} , ΔE_{orb} , etc. (including maintaining the distinction between C_k^{22} and D_k^{22} which, for simplicity, was dropped following equation [A7]). These expressions, however, contain summations over both mode order and fourier coefficients and are thus somewhat involved. We now discuss several approximations which allow for clearer physical understanding of the behavior of and relationship between ΔL , $\Delta E_{tide}^{(r)}$ and ΔE_{orb} .

The dominant contribution to the angular momentum and energy deposited comes from the resonant term in the fourier series, i.e., the integer k for which $\eta_k(m)$ is minimized; we denote this value by k_α . Keeping only this term in the fourier series, the above expressions for ΔL , $\Delta E_{tide}^{(r)}$ and ΔE_{orb} simplify to

$$\Delta L \approx -\frac{8\pi\beta^2}{\Omega_o^2} \sum_n Q_{n22}^2 \omega_{n22}^2 d_{n22} \frac{(D_{k_\alpha}^{22})^2}{[\eta_{k_\alpha}(2)]^2} (2\Omega_* - k_\alpha), \quad (A14)$$

$$\begin{aligned} \Delta E_{tide}^{(r)} \approx & \frac{4\pi\beta^2}{\Omega_o^4} \sum_n Q_{n22}^2 \omega_{n22}^2 d_{n22} \frac{(D_{k_\alpha}^{22})^2}{[\eta_{k_\alpha}(2)]^2} (2\Omega_* - k_\alpha)^2 \\ & + \frac{\pi\beta^2}{\Omega_o^4} \sum_n Q_{n20}^2 \omega_{n20}^2 d_{n20} \frac{(D_{k_\alpha}^{20})^2}{[\eta_{k_\alpha}(0)]^2} k_\alpha^2 \end{aligned}, \quad (A15)$$

and

$$\begin{aligned} \Delta E_{orb} = -\Delta E_{tide}^{(i)} \approx & \frac{4\pi\beta^2}{\Omega_o^4} \sum_n Q_{n22}^2 \omega_{n22}^2 d_{n22} \frac{(D_{k_\alpha}^{22})^2}{[\eta_{k_\alpha}(2)]^2} k_\alpha (2\Omega_* - k_\alpha) \\ & - \frac{\pi\beta^2}{\Omega_o^4} \sum_n Q_{n20}^2 \omega_{n20}^2 d_{n20} \frac{(D_{k_\alpha}^{20})^2}{[\eta_{k_\alpha}(0)]^2} k_\alpha^2 \end{aligned}, \quad (A16)$$

which are the expressions used in the main body of the text. We note that $\eta_k(0)$ and $\eta_k(2)$ will, of course, in general be minimized by different k_α . These simplified expressions are

typically accurate to within ≈ 30 percent in calculating the energy and angular momentum deposited in the star. The only exception is when $\Omega_* \approx \Omega_p$, at which point equations (A14)-(A16) can underestimate the energy and angular momentum deposited by up to a factor of ≈ 5 .

As a final simplification, we note that the modes with the most energy have $|m| = 2$ and $\omega_\alpha^{(i)} \approx 2\Omega_p$, where $\omega_\alpha^{(i)}$ is the mode frequency in an inertial reference frame. This is because, for $k \gtrsim \Omega_p/\Omega_o$, the D_k^{22} are typically larger than the D_k^{20} by at least a factor of a few ($\gtrsim 3$) and so the $m = 0$ mode energies are in general negligible (with the possible exception of when $\Omega_* \approx \Omega_p$). Furthermore, D_k^{22} peaks at $k \approx 2\Omega_p/\Omega_o$ and decreases exponentially for larger k . Thus, modes with $\omega_\alpha^{(i)} \gtrsim 2\Omega_p$, while they have fewer radial nodes and hence larger Q_α , have less energy than modes with $\omega_\alpha^{(i)} \approx 2\Omega_p$ because of the rapid decrease of $D_{k_\alpha}^{22}$ with k_α . Similarly, for $\omega_\alpha^{(i)} \lesssim 2\Omega_p$, not only is $D_{k_\alpha}^{22}$ smaller, but Q_α is also smaller since the modes have more radial nodes.

Thus the dominant contribution to ΔL and ΔE_{orb} comes from the $k_\alpha \approx 2\Omega_p/\Omega_o$ term in the mode summation, which dramatically simplifies the above expression. From equation (A14) we see that $\Delta L > 0$ for $\Omega_* \lesssim \Omega_p$ and $\Delta L < 0$ for $\Omega_* \gtrsim \Omega_p$, indicating that the tidal force causes $\Omega_* \rightarrow \approx \Omega_p$ (which is called pseudo-synchronous rotation). From equations [A14]-[A16] it follows that $\Delta E_{tide}^{(i)} \approx \Omega_p \Delta L$ and $\Delta E_{tide}^{(r)} \approx (\Omega_p - \Omega_*) \Delta L$. These relations show that the energy in the dynamical tide is a frame dependent quantity. Finally, since $\Delta E_{orb} = -\Delta E_{tide}^{(i)} \approx -\Omega_p \Delta L$, we see that $\Delta E_{orb} < 0$ for $\Omega_* \lesssim \Omega_p$ while $\Delta E_{orb} > 0$ for $\Omega_* \gtrsim \Omega_p$ (see Figure 2). The orbital period of a binary system thus increases due to the dissipation of the dynamical tide if $\Omega_* \gtrsim \Omega_p$ since the energy removed from the spin of the star (which is being slowed down by the tidal torque) exceeds the energy deposited in modes.

We now show that the dissipation of the equilibrium tide leads to an analogous relationship among $\dot{E}_{tide}^{(i)}$, $\dot{E}_{tide}^{(r)}$, and τ . For the equilibrium tide, we find it easiest to explicitly sum over the $m = \pm 2$ components in U , in which case

$$U = -V(t) \cos [2(\phi - \phi_{orb}(t) + \Omega_* t)] + V_0(t), \quad (\text{A17})$$

where $V(t) = 2\beta r^2 Y_{2,2}^*(\pi/2, 0) Y_{2,2}(\theta, \phi) / [R(t)/a]^3$ and the $m = 0$ contribution to the tidal potential is given by $V_0(t) = \beta r^2 Y_{2,0}^*(\pi/2, 0) Y_{2,0}(\theta, \phi) / [R(t)/a]^3$. The equilibrium tide represents the hydrostatic response of the primary to the perturbing gravitational force of the secondary and so the time dependence of the equilibrium tide follows that of the tidal gravitational potential. Thus, the mode amplitude for the equilibrium tide, as seen by an observer corotating with the star, is given by (Kumar et al. 1995)

$$A_\alpha = \int d^3x U(\mathbf{r}, t) \delta\rho_\alpha. \quad (\text{A18})$$

Substituting U and A_α into equations (A4) and (A9) it is easy to show that, near periastron, $\dot{E}_{tide}^{(r)} \approx (\Omega_p - \Omega_*) \tau_z$ and $\dot{E}_{tide}^{(i)} \approx \Omega_p \tau_z$, where we have taken $\dot{\phi}_{orb}(t) \approx \Omega_p$ and

$\dot{R}(t) \approx 0$, which are valid near periastron. For highly eccentric orbits, the energy in the equilibrium tide peaks strongly near periastron and so most of the contribution to ΔL and ΔE_{orb} comes from near periastron. Thus, as with the dynamical tide, $\Delta E_{orb} \approx -\Omega_p \Delta L$ for the equilibrium tide.

Appendix B

Neglecting the rotational modification to the equilibrium structure of the star, the perturbed mass and momentum equations, for a rotating star, in the Cowling approximation are

$$\delta\rho + \nabla \cdot (\rho\xi) = 0 \quad (B1)$$

and

$$-\omega^2 \rho\xi = -\nabla\delta p + \delta\rho \mathbf{g} + 2\rho i\omega\xi \times \mathbf{\Omega}_*, \quad (B2)$$

where δ denotes an Eulerian perturbation and we have assumed a time dependence of $\exp(i\omega_\alpha t)$. The Centrifugal force does not appear in equation (B2) because it has no Eulerian perturbation.¹² The components of the momentum equation for adiabatic oscillations can be written as

$$-\omega^2 \rho\xi_r = -\frac{d\delta p}{dr} - \frac{g\delta p}{c_s^2} - N^2\xi_r\rho + 2i\omega\rho\Omega_*\xi_\phi \sin\theta, \quad (B3)$$

$$-\omega^2 \rho\xi_\theta = -\frac{1}{r} \frac{d\delta p}{d\theta} + 2i\omega\rho\Omega_*\xi_\phi \cos\theta, \quad (B4)$$

and

$$-\omega^2 \rho\xi_\phi = -\frac{1}{r \sin\theta} \frac{d\delta p}{d\phi} - 2i\omega\rho\Omega_*(\xi_r \sin\theta + \xi_\theta \cos\theta), \quad (B5)$$

where we have taken $\mathbf{\Omega}_* = \Omega_* \hat{\mathbf{z}}$. In the region of wave propagation $\xi_\phi \sim N\xi_r/\omega$, and thus the buoyancy term in the radial momentum equation is larger than the Coriolis term by a factor of N/Ω_* ; we thus neglect the latter. Away from the equator, $\xi_r \sin\theta \sim (\xi_\theta \cos\theta)\omega/N$ and thus we neglect the radial displacement in the ϕ component of the momentum equation. These approximations constitute the ‘traditional approximation’ (Bildsten et al. 1996; Chapman & Lindzen 1970; Unno et al. 1989) and are only valid when $\omega_\alpha \ll N$ and $\Omega_* \ll N$.

Solving for ξ_θ and ξ_ϕ in terms of δp and taking the perturbed variables to be proportional to $\exp(im\phi)$ we obtain the following coupled radial equations

$$\frac{1}{r^2} \frac{d}{dr}(r^2\xi_r) + \frac{\delta p}{\rho c_s^2} \left[1 - \frac{\lambda c_s^2}{r^2 \omega^2} \right] - \frac{g\xi_r}{c_s^2} = 0, \quad (B6)$$

and

$$\frac{d\delta p}{dr} + \frac{g\delta p}{c_s^2} - \rho(\omega^2 - N^2)\xi_r = 0, \quad (B7)$$

¹² Equivalently, the Centrifugal force evaluated at the perturbed position of the fluid is identically canceled by the equilibrium structure of the star evaluated at the perturbed position.

where the angular eigenfunctions (called the Hough functions) and eigenvalues (λ) are the solutions to the following eigenvalue problem

$$L_q H = -\lambda H, \quad (B8)$$

where

$$L_q = \frac{-m^2}{(1-x^2)(1-q^2x^2)} + \frac{d}{dx} \left[\frac{1-x^2}{1-q^2x^2} \frac{d}{dx} \right] - qm \frac{1+q^2x^2}{(1-q^2x^2)^2}, \quad (B9)$$

where $x = \cos \theta$ and where the angular operator (and thus λ and the Hough functions) depends on the stellar rotation rate and mode frequency through the parameter $q \equiv 2\Omega_*/\omega_\alpha$. We note that, for a fixed $|m|$, $|\omega_\alpha|$, and $|\Omega_*|$, it is the sign of $m\Omega_*/\omega_\alpha$ that determines the effect of the Coriolis force.

Figure (5a) shows λ as a function of $q \equiv 2\Omega_*/\omega_\alpha$ for the even Hough function with the smallest value of λ , which is a generalization of $\ell = 2$. For $m = -2$, $\lambda \rightarrow m^2 = 4$ for $q \gg 1$ and thus the mode structure of the $m = -2$ modes is only weakly modified by the rotation of the star. More detailed discussion of the Hough functions is given in the above references. In what follows, we focus on the aspects of the modified mode structure relevant to tidal excitation.

The overlap integral for a mode can be written as

$$Q_\alpha \equiv Q_{\alpha,r} Q_{angle} = \int dr r^4 \delta\rho_\alpha(r) \int d\Omega H_{\lambda m}^q(\theta) Y_{2m}(\theta, \phi) e^{-im\phi}. \quad (B10)$$

It can easily be shown using a WKB analysis, or verified numerically, that $Q_{\alpha,r}$, the radial contribution to the overlap integral, is only a function of the number of radial nodes of the mode, *i.e.*, for a fixed n , $Q_{\alpha,r}$ is independent of Ω_* , ω_α , λ and m . The overlap of the even Hough function with the smallest value of λ (the generalization of $\ell = 2$) with the quadrupole spherical harmonic, Q_{angle} , is shown in Figure (5b) as a function of q . For $q \lesssim 1$, the associated Legendre polynomials are very good approximations to the Hough functions, but for $q \gtrsim 1$ the Hough functions are concentrated near the equator.

Using the information in Figure (5), there is a simple prescription for calculating g-mode frequencies and overlap integrals of a rotating star in the ‘traditional approximation’. To calculate the frequency of a quadrupole g_n mode, take the value of $q_\alpha = 2\Omega_*/\omega_n^0$ (superscript *o* denotes the value for non-rotating star) and determine λ from Figure (5a). The frequency in the rotating star is, to first approximation, given by $\omega_n^0 \lambda^{1/2} / \sqrt{6}$. This frequency can be used to re-evaluate q_α and in turn λ and ω_α , and this process can be iterated to the desired accuracy. The angular overlap integral, Q_{angle} , can be determined from Figure (5b) using the resulting value of q_α and, since $Q_{\alpha,r}$ is a function of n alone, independent of Ω_* , we obtain Q_α for the g-modes of the rotating star.

REFERENCES

- Bell, J.F., Bessell, M.S., Stappers, B.W., Bailes, M., Kaspi, V.M. 1995, ApJ, 447, L117
- Bildsten, L., Ushomirsky, G., and Cutler, C. 1996, ApJ, 460, 827
- Chapman, S. and Lindzen, R. S. 1970, *Atmospheric Tides* (Dordrecht: Reidel)
- Goldreich, P. and Nicholson, P. D. 1989, ApJ, 342, 1079
- Hut, P. 1981, A & A, 99, 126
- Johnston, S., Manchester, R.N., Lyne, A.G., Bailes, M., Kaspi, V.M., Guojun, Q., and D'Amico, N., 1992, ApJ 387, L37
- Kaspi, V.M., Baile, M., Manchester, R.N., Stappers, B.W., and Bell, J.F. 1996, Nature, 381, 584
- Kaspi, V.M., Johnston, S., Bell, J.F., Manchester, R.N., Bailes, M., Bessell, M., Lyne, A.G., and D'amico, N., 1994, ApJ, 423, L43
- Kumar, P. 1994, ApJ, 428, 827
- Kumar, P., Ao, C. O., and Quataert, E. J., 1995, ApJ, 449, 294
- Kumar, P. and Goodman, J., 1996, 466, 946
- Kumar, P. and Quataert, E. J., 1996,
- Lai, D. 1996, ApJ, 466, L35
- Lai, D., Bildsten, L., and Kaspi, V.M 1995, ApJ, 452, 819
- McConnell, D., McCulloch, P.M., Hamilton, P.A., Ables, J.G., Hall, P.J., Jacka, C.E., and Hunt, A.J., 1991, MNRAS 249, 654
- Press, W.H., and Teukolsky, S.A., 1977, ApJ, 213, 183
- Quataert, E.J., Kumar, P., and Ao, C.O. 1996, ApJ, 463, 284
- Saio, H. and Cox, J.P. 1980, ApJ, 236, 549
- Unno, W., Osaki, Y., Ando, H., Saio, H., and Shibahashi, H., 1989, *Nonradial Oscillations of Stars*, 2nd Ed. (University of Tokyo Press)

Table 1
Parameters for the SMC binary system

Orbital period (P_{orb})	4.421×10^6 s (51.17 days)
e	0.8079
P_{orb}/\dot{P}_{orb}	-4.63×10^5 yr.
$1/ \dot{e} $	$> 1.5 \times 10^5$ yr.
$\Omega_p/2\pi$	3.61 μ Hz
M_*	$\approx 8.8 M_\odot$
R_*	$\approx 6.0 R_\odot$
$\Omega_*/2\pi$	10.1 μ Hz for $\hat{\Omega}_* = 0.5$

Table 2

Frequencies and radiative dissipation times (energy) for the low order quadrupole g-modes of a non-rotating B-star of mass $8.8 M_{\odot}$ and radius $6.0 R_{\odot}$

n (radial nodes)	frequency (μHz)	Γ_{α}^{-1} (yrs)
1	34.66	8.7×10^3
2	23.04	2.5×10^3
3	17.17	1.1×10^3
4	12.58	4.6×10^2
5	11.21	1.6×10^2
6	9.58	47.9
7	8.43	14.5
8	7.56	5.6
9	6.83	2.5
10	6.23	1.1

Figure Captions

FIG. 1.— (a) The energy in the dynamical tide for the B-star of the SMC Binary, as seen by an observer corotating with the B-star ($E_{tide}^{(r)}$), as a function of the B-star’s rotation rate (in units of $\sqrt{GM_*/R_*^3}$). (b) The energy in the dynamical tide for the B-star of the SMC Binary, as seen by an inertial observer ($E_{tide}^{(i)}$). Note that $E_{tide}^{(r)} > 0$ for all rotation rates while $E_{tide}^{(i)} > 0$ for $\Omega_* \lesssim \Omega_p$, i.e., $\hat{\Omega}_* \lesssim 0.2$ (solid line) but $E_{tide}^{(i)} < 0$ for $\Omega_* \gtrsim \Omega_p$ (dashed line). All relevant $\ell = 2$ g-modes of $m = 0, \pm 2$ were included in the calculations. These calculations (as well as those of Fig. 2) were made using the full fourier series expressions for $E_{tide}^{(i)}$ and $E_{tide}^{(r)}$ given in Appendix A.

FIG. 2.— (a) The change in the orbital energy per orbit, ΔE_{orb} , and (b) the resulting orbital evolution timescale, P_{orb}/\dot{P}_{orb} , for the radiative dissipation of the dynamical tide in a rigidly rotating B-star of the PSR J0045-7319 Binary as a function of the B-star’s rotation rate (in units of $\sqrt{GM_*/R_*^3}$); the calculation included all quadrupole g-modes of $m = \pm 2$ as well as $m = 0$. For $\Omega_* \lesssim \Omega_p$, i.e., $\hat{\Omega}_* \lesssim 0.2$, ΔE_{orb} and P_{orb}/\dot{P}_{orb} are negative (solid line) while for $\Omega_* \gtrsim \Omega_p$, ΔE_{orb} and P_{orb}/\dot{P}_{orb} are positive (dashed line); please see the text for a physical explanation of this result.

FIG. 3.— The local radiative dissipation rate for a quadrupole g-mode of frequency $\approx 17\mu\text{Hz}$ for the B-star of the SMC Binary; this is the mode predominantly excited for rapid retrograde rotation of the B-star ($\hat{\Omega}_* = -0.3$). The dissipation peaks near the outer turning point of the mode, which occurs at $r \approx 0.85R_*$, and so the angular momentum and energy of the mode are deposited well beneath the surface of the star.

FIG. 4.— The adiabatic energy flux in a g-mode of the B-star in the SMC Binary for rigidly (dashed line) and differentially rotating (solid line) stars which have the same rotation frequency in the interior. The differential rotation is centered at $r \approx 0.8R_*$, occurs over a width of $\approx 0.1R_*$, and is such that the minimum wave frequency (which is $\approx 17\mu\text{Hz}$ in the core) is $\approx 1\mu\text{Hz}$ at $r \approx 0.8R_*$. The small wavelength in the differentially rotating layer implies that the mode dissipation is strongly enhanced. Note that energy flux is nearly constant across the differentially rotating layer, or in other words the differential rotation does not significantly reflect the wave.

FIG. 5.— (a) The smallest value of the angular eigenvalue λ as a function of $q \equiv 2\Omega_*/\omega_\alpha$ for even parity modes (these are the generalization of the $\ell = 2$ modes for a rotating star and so $\lambda \rightarrow \ell(\ell + 1) = 6$ as $q \rightarrow 0$). (b) Q_{angle} , the overlap of the angular eigenfunction in the rotating star with the quadrupole spherical harmonic, for the same modes as part (a). Since the radial contribution to the overlap integral is, for a fixed number of radial nodes, independent of Ω_* , Q_{angle} give the variation of the overlap integral with the stellar rotation rate.

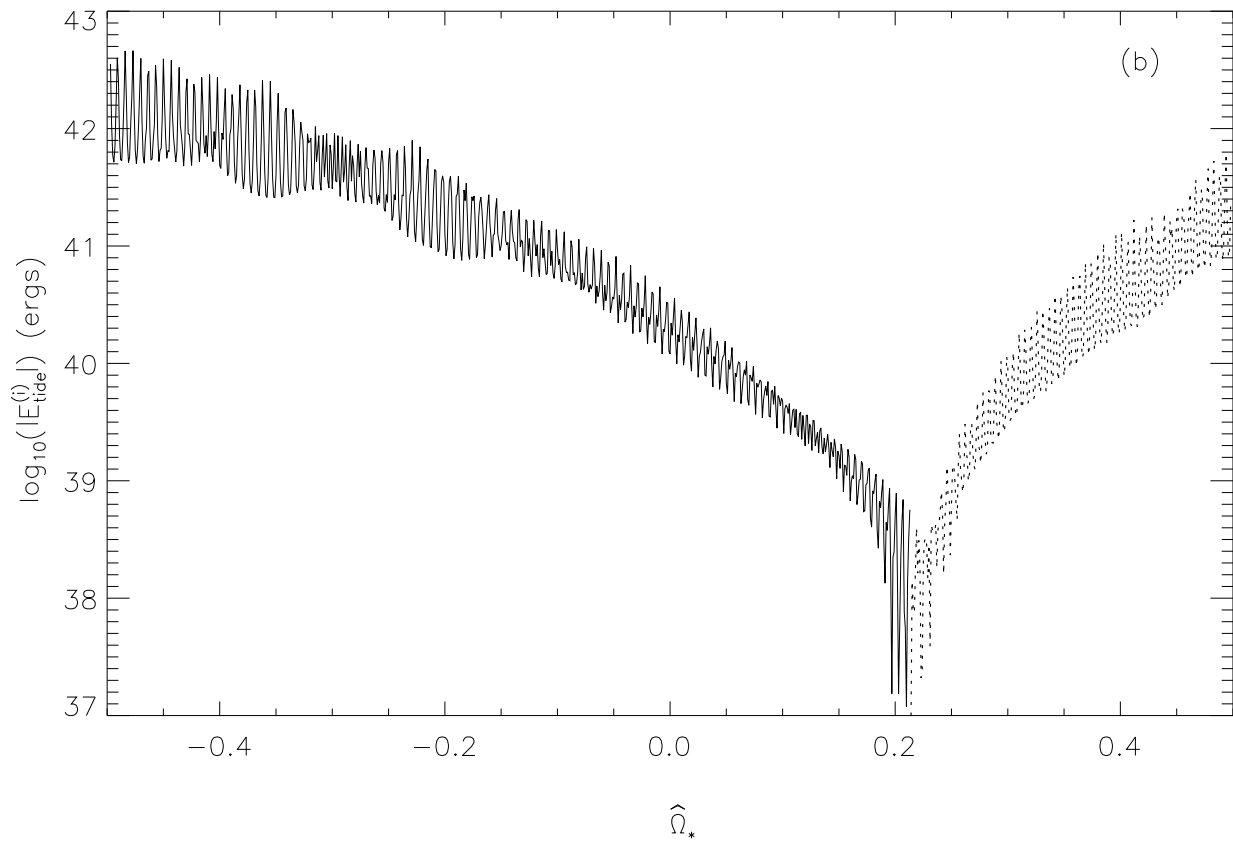
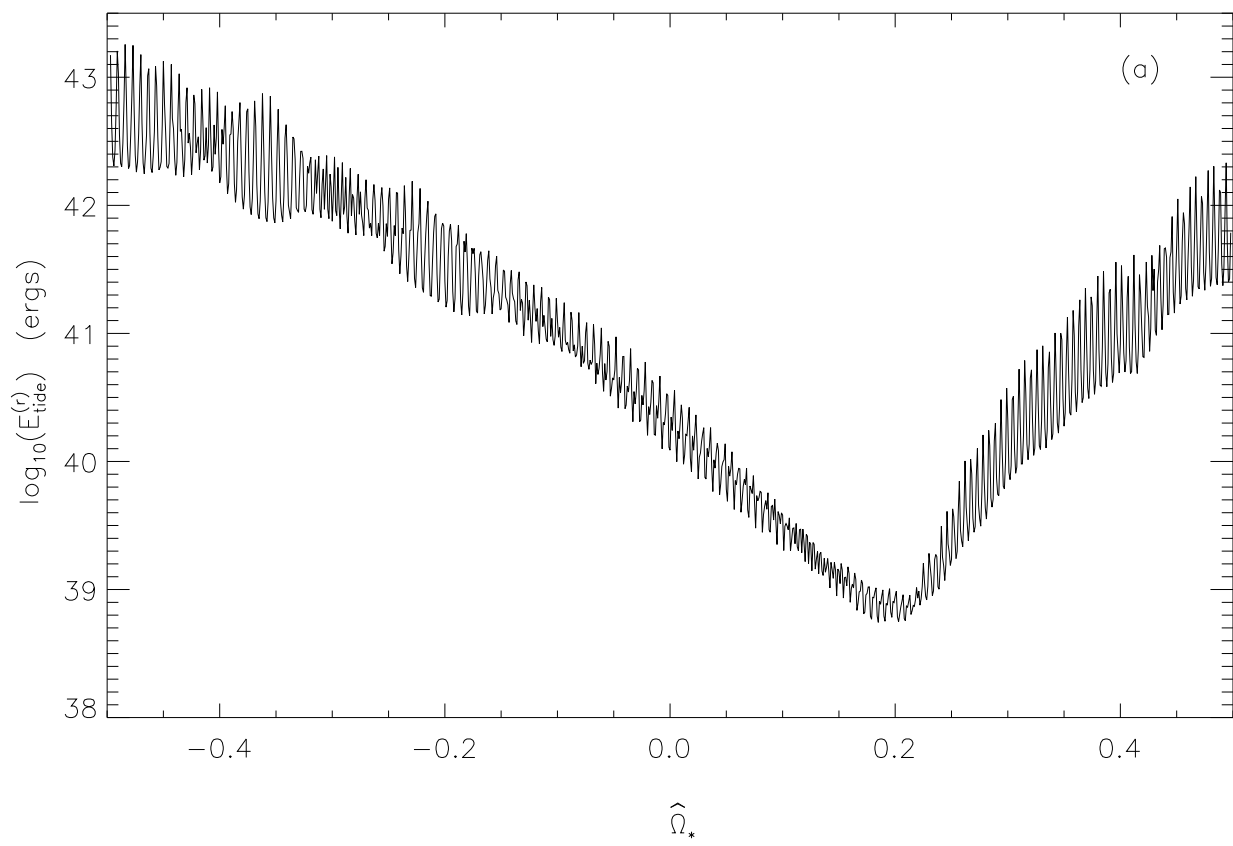


Figure 1

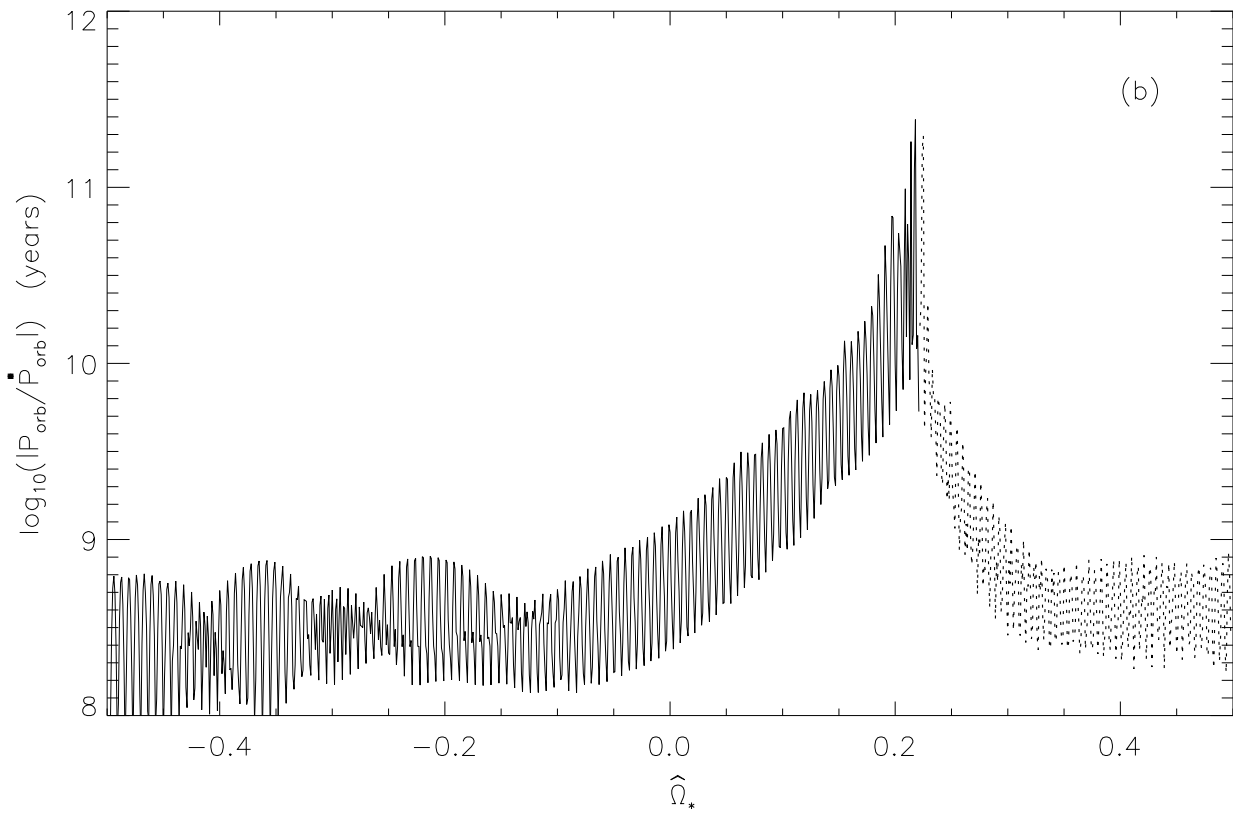
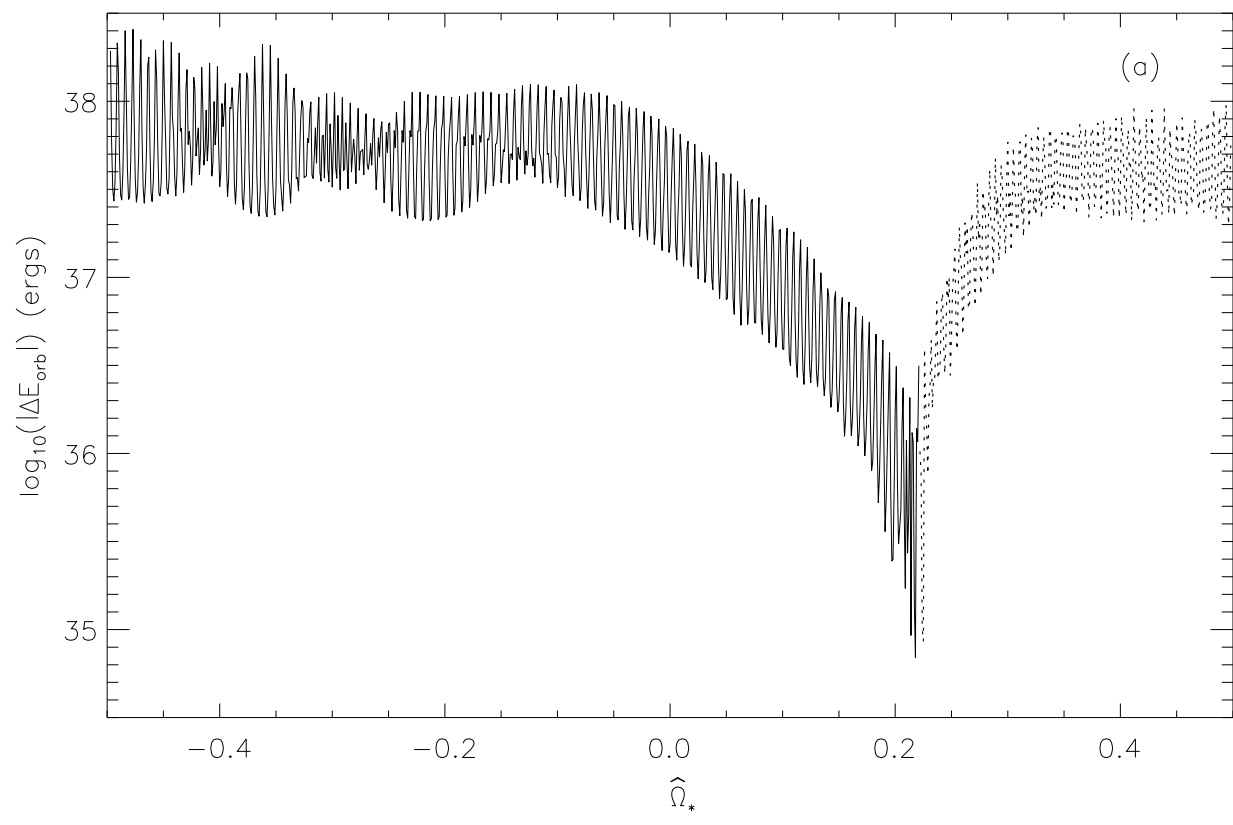


Figure 2

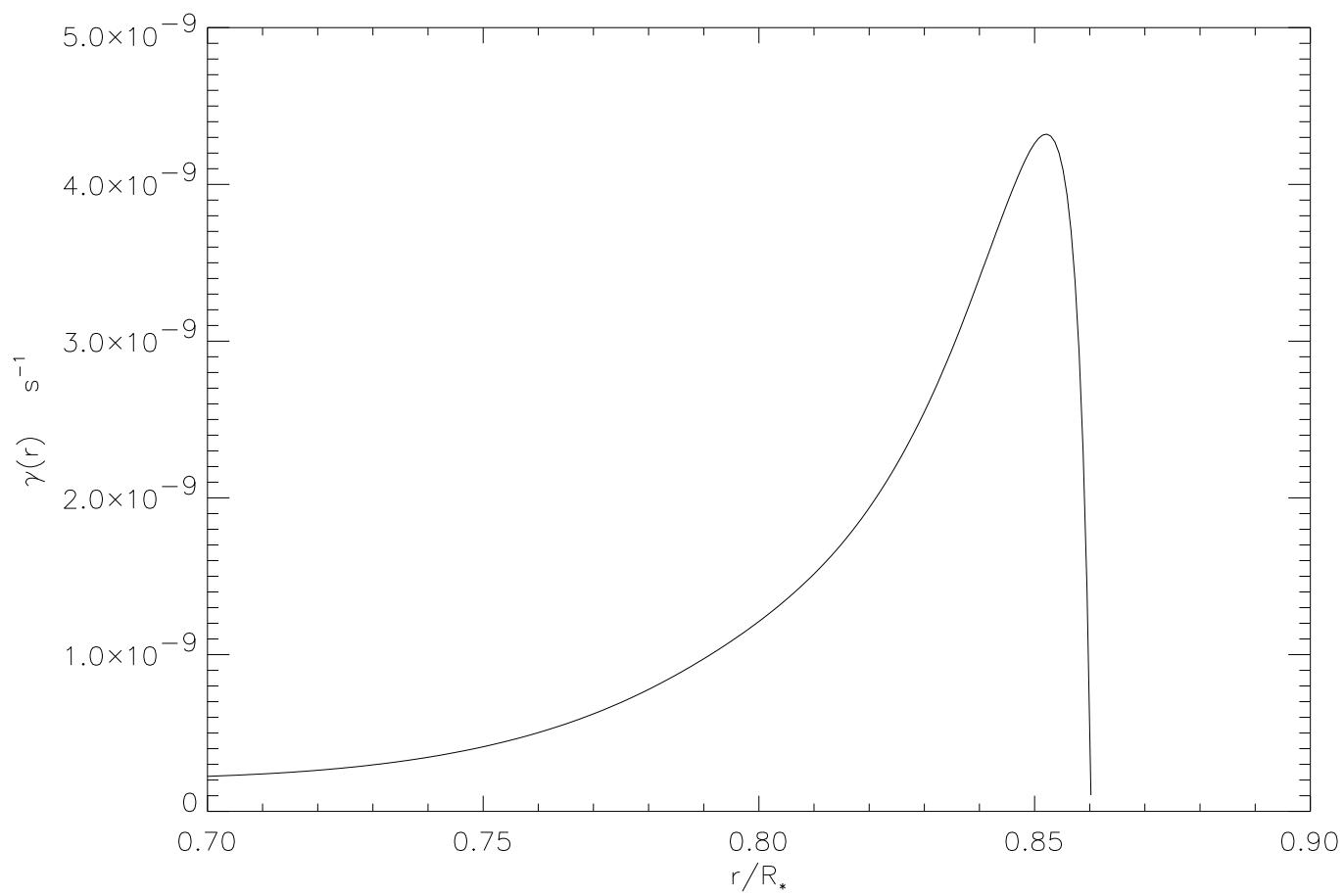


Figure 3

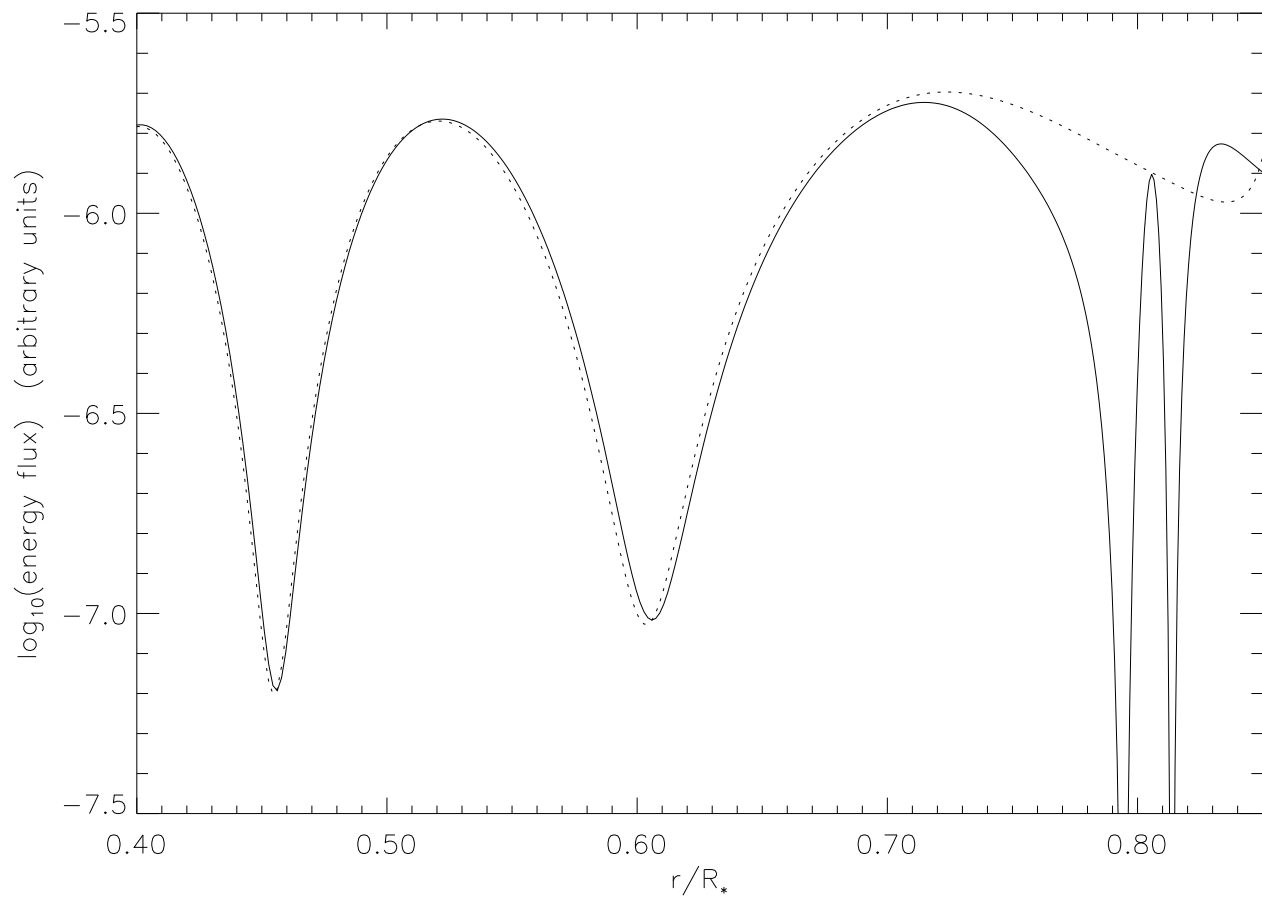


Figure 4

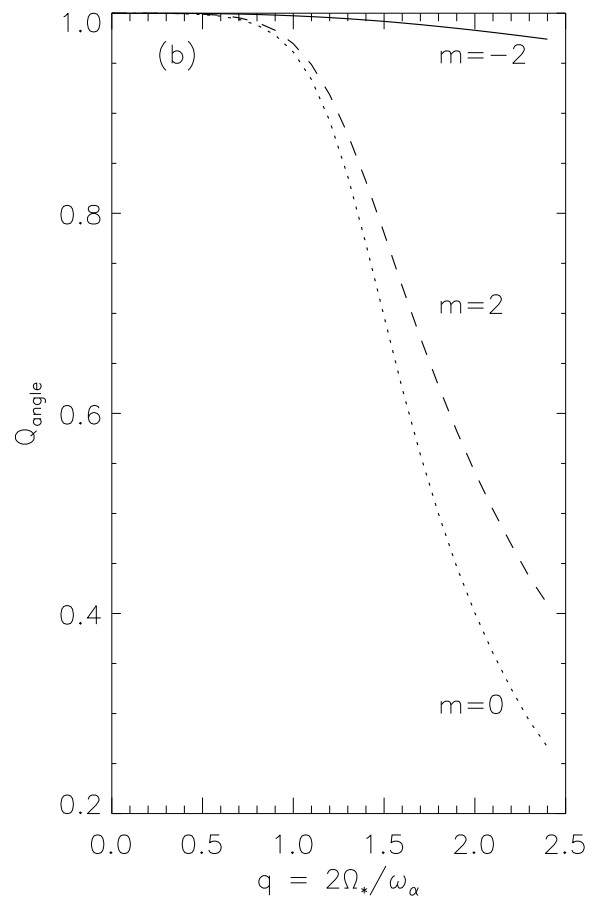
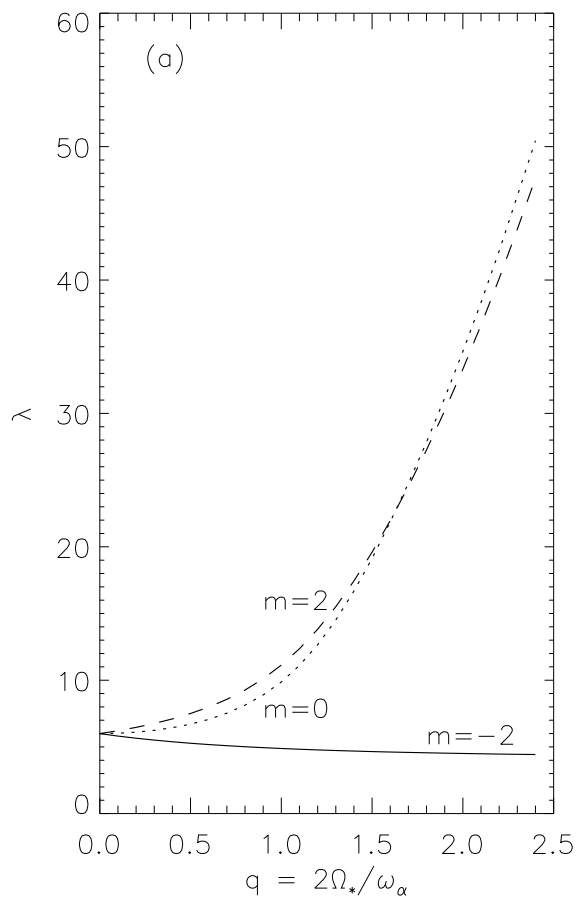


Figure 5